Journal of Systems Engineering and Electronics
Vol. 33, No. 1, February 2022, pp.97 – 104

Analysis of reflected signal of quad rotor UAV based on model fitting in mobile communication system

LI Xiaohui[1,2,*], FANG Cong[1], and FAN Tao[1]

1. School of Telecommunication Engineering, Xidian University, Xi'an 710071, China;
2. Guangzhou Institute of Technology, Xidian University, Guangzhou 510555, China

Abstract: In view of the many scenes of unmanned aerial vehicle (UAV) detection, a third-party signal source is used to design a receiver to monitor the UAV. It is of great significance to understand the reflection of the signal illuminating the UAV. Taking the communication base station (BS) signal as the third-party signal source, and considering the complete transmission link, reflection changes and loss fading of the communication signal, this study conducts model fitting for irregular UAV targets, simplifying complex targets into a combination of simple targets. Furthermore, the influence of the dielectric constant of the target surface and the signal irradiation angle on the signal reflection is analyzed. The analysis shows that the simulation results of this model fitting method are consistent with the results of other literature, which provides theoretical support for the detection of low and slow small targets such as UAVs.

Keywords: mobile communication signal, quad rotor unmanned aerial vehicle (UAV), signal reflection, model fitting.

DOI: 10.23919/JSEE.2022.000011

1. Introduction

In recent years, with the rapid development of low altitude, slow speed, small (LSS) unmanned aerial vehicles (UAVs), a great threat has formed to important target air defense safety [1]. Thus UAV monitoring in low-altitude environments has become more and more important. The monitoring methods using images, audio, and radar have certain deficiencies [2]. Nalamait et al. and Srigrarom et al. used video to detect UAVs, but video images were easily affected by bad weather [3,4]. An acoustic monitoring method was proposed in [5−7], but the acoustic signal susceptible to noise emitted from the UAV itself. Various radar monitoring schemes were proposed, but radar monitoring has high technical difficulties and high cost [8−10].

Therefore, the use of signals emitted by third-party signal sources to monitor UAV provides a new idea. Taking a mobile communication base station (BS) as an example. The mobile communication BS is widely distributed and it continuously sends communication signals. They establish a stable signal link with mobile stations (such as mobile phones). These characteristics have natural advantages. These signals have high radiation power and unidirectional low-altitude coverage, making it easy to detect low-altitude targets. In addition, the continuous and broadband bandwidth of the communication signal sent by the BS can continuously detect slow targets and small targets [11]. And it is proved that it is feasible to use digital TV broadcast signals to detect UAV [12,13]. It is of great significance to study the reflection of communication signals irradiated by the UAV and can provide a theoretical basis for monitoring the UAV. Among existing research, there is research on global navigation satellite system (GNSS) reflected signals. It is used to realize the detection of soil moisture[14−16], the detection of vegetation existence [17], ice/snow thickness [18], and the detection of traffic flow [19].

In the use of UAVs, the quad rotor UAV has the highest efficiency and it is easy to use. At the same time, the general quad rotor UAV has a slow flight speed, relatively small size, and low flying height, which belongs to the LSS's target [20], so the quad rotor UAV is chosen as the experimental object. It is a complex target in itself, and the target is simplified by model fitting, and the reflection of the communication signal on its surface is studied. Xie et al. analyzed the reflected signal after irradiating the target spacecraft based on the signal transmitted by the GNSS small satellite, and established a small satellite cylindrical model based on the characteristics of the small satellite [21].

The monitoring system is composed of a transmitting

Manuscript received December 02, 2020.
*Corresponding author.
This work was supported by the State Major Research and Development Project (2018YFB1802004) and the State Key Laboratory of Air Traffic Management System and Technology (SKLATM201807).

BS, a target for detection, and receiving equipment. The transmitting BS continuously radiates signals outward, and the receiving equipment receives the direct wave signal transmitted by the transmitting BS and the multipath and clutter signals reflected from the ground and buildings. If there is a target UAV, it will also receive the reflected signal of the target UAV.

The mobile communication BS described here includes 3rd-generation (3G), long term evolution (LTE) and 5th-generation (5G) transmitting BS. The radiated energy is relatively small, resulting in a smaller target echo power. However, when the signal frequency is high or in the 5G micro area, the signal transmission will be enhanced when the signal meets the mirror reflection of the object [22]. In this paper, first of all, a brief description of the propagation fading characteristics of the signal is made. After taking the quad rotor UAV as the object, it conducts a model pseudo-cooperative reflection analysis, and considers that the LSS's target receives the reflected signal power received by the BS in the case of secular reflection. Finally, the signal reflection under different influence factors is simulated and analyzed.

2. Fading characteristics of signal propagation

The mobile communication signal is essentially an electromagnetic wave, with diverse propagation mechanisms. Generally, the BS transmits a signal in the free space which is radiated as electromagnetic waves through the atmosphere to the surroundings. A system architecture diagram is given in Fig. 1. When the antenna of the transmitting BS is an isotropic antenna, the transmission power of the signal is P_t, and the signal propagates through the atmosphere at a distance R. The power density P'_R is

$$P'_R = \frac{P_t}{4\pi R^2}. \tag{1}$$

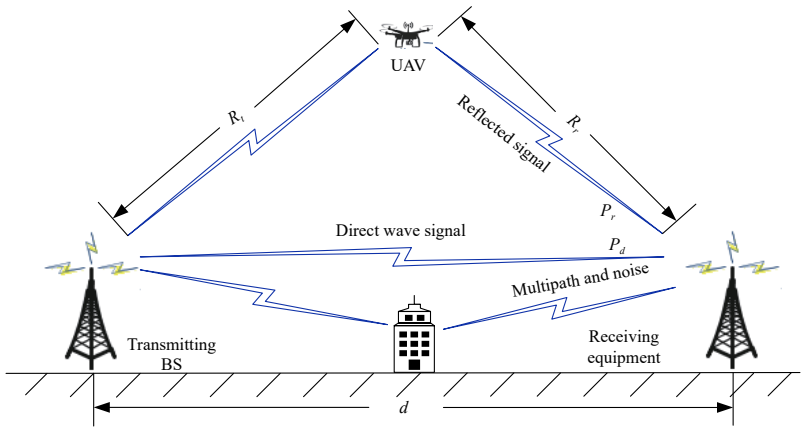

Fig. 1 System architecture diagram

When the transmitting antenna is a directional antenna and the antenna gain is G_t, the power density P_R of the transmitted signal passing through the distance R is

$$P_R = \frac{P_t G_t}{4\pi R^2}. \tag{2}$$

If the distance of the target from the transmitting BS is R, the reflected signal power of the target is

$$P_{re} = P_R \sigma = \frac{P_t G_t \sigma}{4\pi R^2}. \tag{3}$$

Among them, σ is the reflection cross-sectional area of the target, which is a physical quantity measuring the intensity of the echo generated by the signal illuminating the target, and can be used to indicate the reflection intensity of the target to the signal.

As shown in Fig. 1, the distance between the transmitting BS and the target UAV is R_t, the distance between the receiving equipment and the target UAV is R_r. d is the distance between the transmitting BS and the receiving equipment. According to the formula of the relationship between the antenna gain and the effective area [23] and (3), the power of the target reflected signal received is

$$P_r = \frac{P_t G_t \sigma}{4\pi R_t^2} \cdot \frac{1}{4\pi R_r^2} \cdot \frac{G_r \lambda^2}{4\pi} = \frac{P_t G_t G_r \lambda^2 \sigma}{(4\pi)^3 R_t^2 R_r^2} \tag{4}$$

where λ is the signal wavelength, G_t and G_r are the antenna gains of the transmitter and receiver respectively.

The direct wave signal power P_d received by the receiving end is

$$P_d = \frac{P_t G_t}{4\pi d^2} \cdot A_r = \frac{P_t G_t}{4\pi d^2} \cdot \frac{G_r \lambda^2}{4\pi} = \frac{P_t G_t G_r \lambda^2}{(4\pi)^2 d^2}. \tag{5}$$

3. Model fitting and reflection analysis of quad rotor UAV

A common quad rotor UAV is shown in Fig. 2(a). It con-

sists of a cube-like fuselage and propellers distributed at it are four vertices. Therefore, when conducting signal reflection research, this article divides the quad rotor UAV into two parts, consisting of a rectangular parallelepiped and propellers on four vertices. These two parts are used as models for fitting, as shown in Fig. 2(b). Therefore, when performing signal reflection analysis, the cuboids and propeller can be analyzed separately, and then the reflection of the quad copter UAV under the mobile communication signal can be studied.

(a) Actual UAV

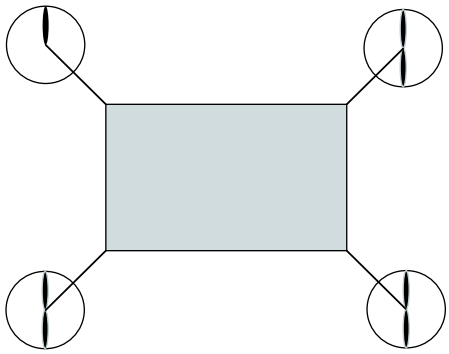

(b) UAV after model fitting

Fig. 2 UAV model fitting comparison

As a rotating object, the reflection of the UAV propeller is different from that of the fuselage when the signal irradiates on its surface. The reflection is more complex and related to multiple factors. The reflection formula of aircraft propeller to electromagnetic signal was given in [24]. However, according to the characteristics of the propeller of the quad rotor UAV, the reflection formula given is rewritten in combination with actual characteristics. The time domain formula of the reflection signal is

$$v_r(t)=\sum_{n=0}^{N-1}A_rL\operatorname{sinc}\alpha_n\exp\left[\mathrm{j}\left(\omega_c t-\frac{4\pi}{\lambda}\beta_n\right)\right]. \tag{6}$$

Among them, α_n and β_n are

$$\alpha_n=\frac{4\pi}{\lambda}-\frac{L}{2}\cos\theta\sin\left(\omega_r t+\frac{2\pi n}{N}\right), \tag{7}$$

$$\beta_n=R'+vt+\frac{L}{2}\cos\theta\sin\left(\omega_r t+\frac{2\pi n}{N}\right). \tag{8}$$

Physical meanings of parameters are shown in Table 1.

Table 1 Parameter description for (6), (7) and (8)

Parameter	Description
A_r	Scale factor
L/m	Propeller blade length
N	Number of propeller blades
R'/m^2	Range of propeller blades
t/s	Time
$v/\mathrm{m}\cdot\mathrm{s}^{-1}$	UAV speed
λ/m	Transmitting signal wavelength
θ/rad	Angle between the plane of rotation and the line of sight from the transmitting BS to the centre of rotation
$\omega_c/\mathrm{rad}\cdot\mathrm{s}^{-1}$	Angular frequency of transmitted signal
$\omega_r/\mathrm{rad}\cdot\mathrm{s}^{-1}$	Rotating angle frequency of propeller blade

In the high frequency band, the reflection of electromagnetic wave signal is mainly dependent on the shape of the object and the amplitude, phase, and polarization of the incident wave at the incident point [25]. Therefore, the reflection area can be used to characterize the reflection of the signal on the object. However, for a complex target, its reflection area is related to secular reflection, edge diffraction, tip diffraction, crawling wave diffraction, traveling wave diffraction, and electromagnetic mutation induced diffraction. For a cuboid belonging to a simple regular target, it is relatively simple to calculate the reflection area of the signal encountering the regular object. The reflection area of the cuboids can be replaced by the optical reflection cross-section area. Therefore, using the physical optics method, the reflection cross-sectional area of the cuboids [26] is

$$\sigma=\frac{4\pi D^4}{\lambda^2}\cdot\cos^2\theta\cdot\frac{\sin^2 b_1}{b_1^2}\cdot\frac{\sin^2 b_2}{b_2^2} \tag{9}$$

where D is the length of either side. Among them

$$\begin{cases} b_1=kD\sin\theta\cos\varphi \\ b_2=kD\sin\theta\sin\varphi \end{cases} \tag{10}$$

where k is the wave number, $k=2\pi/\lambda$, and θ and φ are the elevation and azimuth of the incident signal respectively, as shown in Fig. 3.

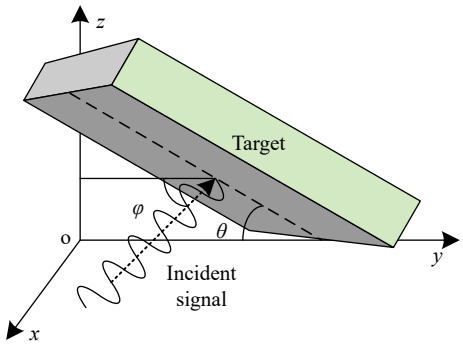

Fig. 3 Angle between incident signal and cube

When the signal is reflected by the medium, the horizontal polarization Fresnel reflection coefficient Γ_H and vertical polarization Fresnel reflection coefficient Γ_V can be calculated based on the reflection law [27]. The Fresnel reflection coefficient is related to the incident angle n of the radio wave and the dielectric constant ε of the surface of the medium [28]. The schematic diagram of the angle between the signal and the target is shown in Fig. 4. We can get the following results:

$$\Gamma_V = \frac{n\sin\varphi - \sqrt{n-\cos^2\varphi}}{n\sin\varphi + \sqrt{n-\cos^2\varphi}}, \tag{11}$$

$$\Gamma_H = \frac{\sin\varphi - \sqrt{n-\cos^2\varphi}}{\sin\varphi + \sqrt{n-\cos^2\varphi}}. \tag{12}$$

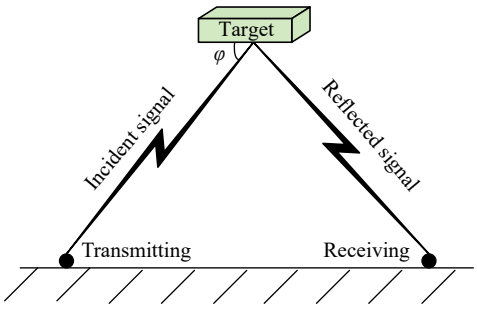

Fig. 4 Schematic diagram of the angle between the incident signal and the target

When the electromagnetic signal meets the target, part of the electromagnetic signal will be reflected. The shortest path point of the transmitting BS signal to the receiving equipment through the reflection point is called the mirror reflection point [29] on the surface of the UAV. The formula for secular reflection was obtained in [30]. The secular reflection coefficient is

$$\rho_s = \mathrm{e}^{-4\pi\Theta}\cdot|\Gamma_V| \tag{13}$$

where Θ is the smoothness of the surface of the reflected object.

At the same time, the diffuse reflection coefficient ρ_d can be obtained from the secular reflection coefficient:

$$\rho_d = \sqrt{1-\left(\frac{\rho_s}{|\Gamma_V|}\right)^2}\cdot|\Gamma_V|. \tag{14}$$

Given the incident angle and wavelength of the signal, the secular reflection loss L_{sr} and diffuse reflection loss L_{dr} will be produced when the signal meets the target.

$$L_{sr} = 10\lg\frac{1}{\rho_s^2} \tag{15}$$

$$L_{dr} = 10\lg\frac{1}{\rho_d^2} \tag{16}$$

According to the definition of the secular reflection coefficient, the amplitude of the reflected wave is divided by the amplitude of the incident wave. Considering the square relationship between the instantaneous power of the signal and the amplitude of the signal, as well as the secular reflection loss of the signal during reflection, we can get the reflected signal power of the target

$$\frac{P'_{re}}{P_R} = \rho_s^2. \tag{17}$$

P'_{re} can be concluded by combining (2) and (15). Signal power P_r' of the target reflection received by the receiving equipment under secular reflection can be obtained:

$$P'_r = \frac{\rho_s^2 G_r \lambda^2\left(\dfrac{P_t G_t}{4\pi R_t^2}\right)}{(4\pi R_r)^2} - L_{sr}. \tag{18}$$

The receiving equipment receives the direct wave signal and the target reflection signal, where the target reflection signal includes the reflection signal of the regular cuboids and the reflection signal of the quad rotor propeller. Thus it can be expressed in a time domain as

$$S_d(t) = Ar(t) + kr(t-\tau)\mathrm{e}^{\mathrm{j}2\pi ft} + 4v'_r(t) + n(t) \tag{19}$$

where A is the amplitude gain of the direct wave signal. $r(t)$ is the signal emitted by the transmitter. k, τ, and f respectively represent the signal gain, time delay, and Doppler shift of the direct wave signal reflected by a LSS's target. $v'_r(t)$ is the time-domain signal received by the receiving equipment after the reflection loss of the quadrotor propeller. $n(t)$ is the noise signal.

4. Simulation and analysis

In the mobile communication network, the signal transmitted by the mobile communication BS irradiates the communication area covered by the BS. When the UAV target passes through the signal irradiation area, it will reflect the mobile communication signal. The receiving

equipment receives the reflected signal. The reflected signal is not only related to the shape and material of the UAV, but also to the angle of the incident signal irradiating the UAV and the equivalent reflection cross-sectional area of the UAV. Although the effective reflection area of the UAV is much smaller than that of the ground, the surface of the UAV is smooth and much less rough than that of the ground.

4.1 Reflection coefficient

The Fresnel reflection coefficient is related to the angle at which the signal illuminates the surface of the object and the dielectric constant of the object surface. The expressions of the dielectric constant of different substances are different. When the signal frequency is less than 100 GHz, the dielectric constant of the insulator n is a real number [31]. Therefore, when the dielectric constant is constant, the Fresnel reflection coefficient will change with different incident angles, resulting in the change of the specular reflection coefficient.

Fig. 5 shows that when the angle between the incident signal and the UAV is larger, the Fresnel reflection coefficient is larger, but the specular reflection coefficient is not only related to the incident angle but also to the dielectric constant of the object.

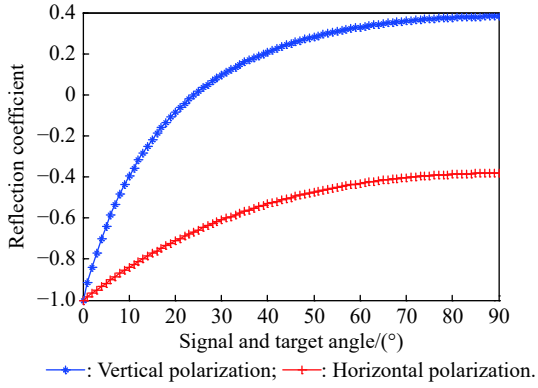

Fig. 5 Fresnel reflection coefficient at different angles

It can be seen from Fig. 6 that the reflection on the surface of the object with different dielectric constants is different, and the dielectric constant of air is 1 [32], indicating that reflection will not occur at any angle. The higher the dielectric constant is, the better the reflection effect will be. When the specular reflection coefficient is 0, it means that the electromagnetic wave signal does not reflect when it reaches the interface of the medium. When the dielectric constant is 1, (11) and (12) are always equal to 0. The incident angle is called Brewster angle because the dielectric constant of different materials and the polarization mode of electromagnetic wave signal lead to the maximum absorption of electromagnetic wave on the surface of the object, and the reflection effect is the worst. When the dielectric constants are 10 and 100, the Brewster 0 angles are 17.55° and 5.71° respectively.

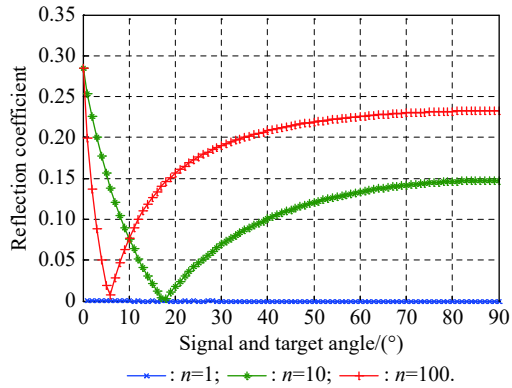

Fig. 6 Specular reflection coefficient of signal and target for different angles

When the signal frequency is less than 100 GHz and the metal is irradiated, the dielectric constant of the metal is very large, so the metal is more likely to absorb electromagnetic waves. Induced currents are generated inside the metal. These induced currents will generate scattered fields, so the reflection effect is better.

Fig. 7 is the curve of the signal-to-noise ratio (SNR) with the distance of the reflected signal in the case of specular reflection. The simulation parameters are shown in Table 2.

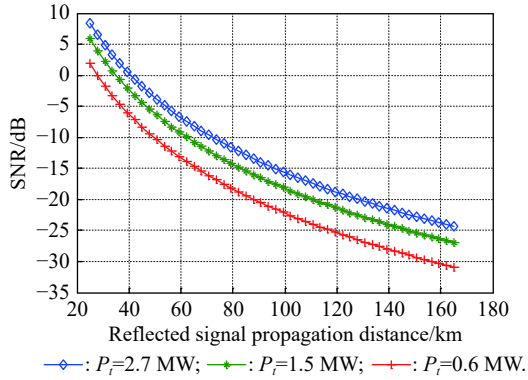

Fig. 7 SNR with distance under specular reflection

Table 2 Simulation parameters of Fig.7

Parameter	Value
Frequency/GHz	3
Transmit antenna gain/dB	45
Receive antenna gain/dB	30
Bandwidth/MHz	20
System loss/dB	6

When the reflected signal travels a certain distance, the greater the transmit power of the transmitting BS, the greater the SNR of the reflected signal received by the receiving equipment. At the same time, as the propagation distance increases, the SNR of the reflected signal received by the receiving equipment becomes smaller.

According to Fig. 8, when the signal encounters the mirror reflection of the target surface, the SNR of the reflected signal received by the receiving equipment will decrease by about 14 dB at the same distance.

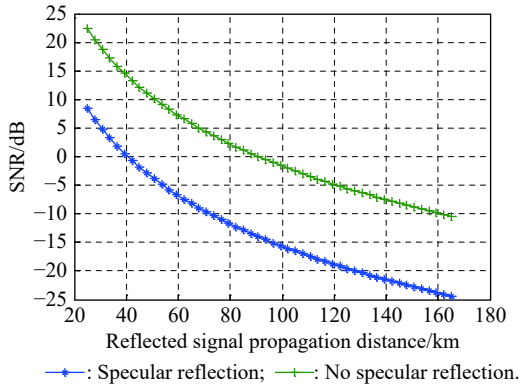

Fig. 8 SNR curve with distance

4.2 Target reflection cross section

The reflection cross-sectional area of the target represents the reflection effect of the object on the signal. In the model in Section 3, the volume of the simulation object is set as 40 cm×40 cm×16 cm, and the relative dielectric constant is 3. The reflection cross-section of the target at different frequencies and angles is verified as shown in Fig. 9. Fig. 9(a) shows the variation curve of the reflection cross-section of the target at different frequencies and angles. Local amplification is shown in Fig. 9(b).

When the signal frequency is 100 MHz, the wavelength is 300 cm, which is much larger than the size of the target object. When the signal frequency is 1 GHz, the wavelength is 30 cm, which is similar to the size of the target object. When the signal hits the surface of the target object, if the signal wavelength is smaller than the target size, reflection occurs, and the target reflection cross-sectional area is large. If the wavelength of the signal is much larger than the size of the object, the object is a small object relative to the signal wavelength. Not only reflection but also scattering occurs, which makes the target reflection cross-sectional area smaller.

Due to the influence of the signal frequency and the target material, a critical angle and the minimum reflection cross-sectional area will be obtained when the signal illuminates the target model. When the object surface dielectric constant is 3 and the signal frequency is 900 MHz, the critical angle is about 65°. When the signal frequency is 1 GHz, the critical angle is about 60°. At this time, the reflection effect of the electromagnetic wave signal on the object surface is the worst. When the angle between the electromagnetic wave signal and the target object is 90°, it indicates that the signal illuminates the target surface vertically, and the reflection cross-sectional area of the target model is the largest. This shows that the reflection effect is also the best when the signal illuminates the surface of the target model vertically. However, when the signal frequency is 100 MHz, the critical angle disappears since the signal wavelength is much larger than the target size. Moreover, as the angle of the signal illuminating the target object increases, the reflected cross-sectional area increases.

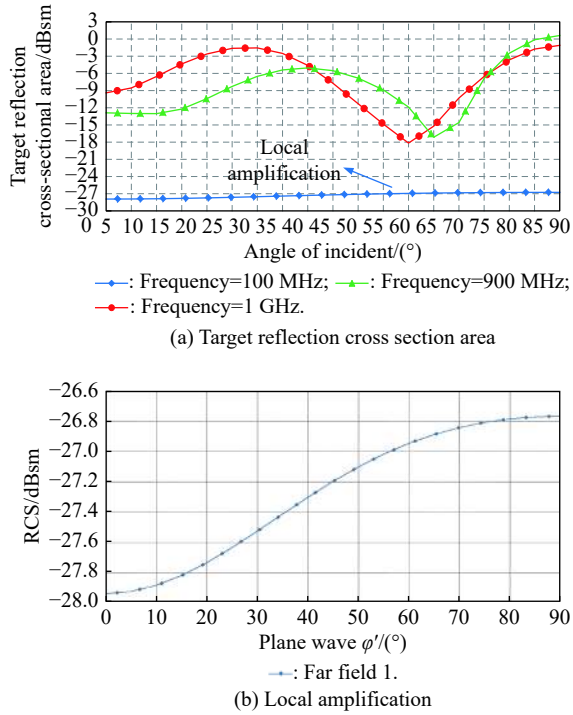

Fig. 9 Target reflection cross section area with different signal frequencies

In [33], the results of measuring the UAV reflection cross-sectional area at different frequencies in a microwave anechoic chamber were given. Fig. 9 mainly focuses on the change of the UAV reflection cross-sectional area at different incident angles at the same frequency, and the range is from −30 dBsm to 0 dBsm. The range of literature [33] at the same frequency is from −25 dBsm to −5 dBsm. This article considers both specular reflection and UAV propeller reflection. Thus at different angles, it will be slightly larger or smaller.

Fig.10 shows that under different target reflection cross-section areas, when the target reflection cross-section is larger, the SNR of the signal received by the BS of the re-

ceiving equipment is also high. When the target reflection cross-sectional area differs by 10 dBsm, the difference in SNR at the same distance is also about 10 dB.

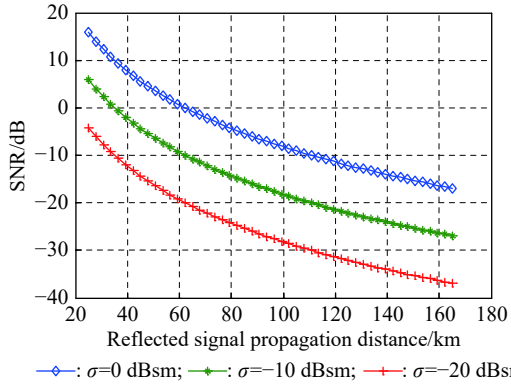

Fig. 10 Variation curve of SNR with reflected signal propagation distance with different σ

5. Conclusions

In this paper, a quad rotor UAV is used as the model fitting to study its reflection based on the electromagnetic wave communication signal transmitted by the mobile communication BS. The reflection of the signal when irradiated to targets with different dielectric constants at different angles is analyzed. The analysis indicates that under the influence of factors such as signal frequency and target surface material, the reflected signal of the signal irradiated to the target has a critical angle and has poor reflection effect. If the specular reflection of the signal on the target surface is considered, the SNR of the receiving equipment will decrease. The simulation results are cosistent with existing literature. At the same time, it is verified that the best reflection effect occurs when the signal illuminates the target vertically. Therefore, in order to increase the maximum detectable distance, it is not only necessary to increase the SNR or the antenna gain of the transmitting BS, but also to consider the angle and frequency of the signal from the transmitting BS.

References

[1] LI M, SHAO J Q, LIU C C, et al. Threat and detection technology of low and slow small drone. Police Technology, 2019, 2: 71–74. (in Chinese)

[2] FU H, ABEYWICKRAMA S, ZHANG L, et al. Low-complexity portable passive drone surveillance via SDR-based signal processing. IEEE Communications Magazine, 2018, 56(4): 112–118.

[3] NALAMATI M, KAPOOR A, SAQIB M, et al. Drone detection in long-range surveillance videos. Proc. of the 16th IEEE International Conference on Advanced Video and Signal Based Surveillance, 2019. DOI: 10.1109/AVSS.2019.8909830.

[4] SRIGRAROM S, HOE CHEW K. Hybrid motion-based object detection for detecting and tracking of small and fast moving drones. Proc. of the International Conference on Unmanned Aircraft Systems, 2020: 615–621.

[5] NIJIM M, MANTRAWADI N. Drone classification and identification system by phenome analysis using data mining techniques. Proc. of the IEEE Symposium on Technologies for Homeland Security, 2016. DOI: 10.1109/THS.2016.7568949.

[6] BUSSET J. Detection and tracking of drones using advanced acoustic cameras. Proceedings of SPIE, 2015, 9647: 96470F-1–96470F-8.

[7] BENYAMIN M, GOLDMAN G H. Acoustic detection and tracking of a class I UAS with a small tetrahedral microphone array. Adelphi: Army Research Lab, 2014.

[8] DROZDOWICZ J. 35 GHz FMCW drone detection system. Proc. of the 17th International Radar Symposium, 2016. DOI: 10.1109/IRS.2016.7497351.

[9] KLARE J, BIALLAWONS O, CERUTTI-MAORI D. Detection of UAVs using the MIMO radar MIRA-CLE Ka. Proc. of the 11th European Conference Synthetic Aperture Radar, 2016: 1–4.

[10] MOSES A, RUTHERFORD M J, VALAVANIS K P. Radar-based detection and identification for miniature air vehicles. Proc. of the IEEE International Conference on Control Applications, 2011: 933–940.

[11] FANG G, YI J X, WAN X R, et al. Experimental research of multi-static passive radar with a single antenna for drone detection. IEEE Access, 2018, 6: 33542–33551.

[12] KIM S, NOH Y H, LEE J, et al. Electromagnetic signature of a quadcopter drone and its relationship with coupling mechanisms. IEEE Access, 2019, 7: 174764–174773.

[13] LI Y C, WANG X D, DING Z G. Multi-target position and velocity estimation using OFDM communication signals. IEEE Trans. on Communications, 2020, 68(2): 1160–1174.

[14] CHEW C C, SMALL E E. Soil moisture sensing using spaceborne GNSS reflections: comparison of CYGNSS reflectivity to SMAP soil moisture. Geophysical Research Letters, 2018, 45(9): 4049–4057.

[15] HYUNGLOK K, VENKAT L. Use of cyclone global navigation satellite system (CyGNSS) observations for estimation of soil moisture. Geophysical Research Letters, 2018, 45(16): 8272–8282.

[16] VORONOVICH A. Numerical simulations of the soil moisture retrieval by measuring angular dependence of the reflection coefficient. Proc. of the IEEE International Geoscience and Remote Sensing Symposium, 2019: 3566–3569.

[17] SMALL E E, LARSON K M, BRAUN J J. Sensing vegetation growth with reflected GPS signals. Geophysical Research Letters, 2010. DOI: 10.1029/2010gl042951.

[18] RODRIGUEZ-ALVAREZ N, AGUASCA A, VALENCIA E, et al. Snow thickness monitoring using GNSS measurements. IEEE Geoscience and Remote Sensing Letters, 2012, 9(6): 1109–1113.

[19] YANG L, YANG D K, ZHU Y L, et al. Traffic flow detection using GNSS-R signals. Acta Geodaetica et Cartographica Sinica, 2018, 47(3): 370–375. (in Chinese)

[20] ZHANG J W, GUO H M. Net cast interception system research aimed at low small slow target. Computer Engineering and Design, 2012, 33(7): 2874–2878.

[21] XIE J, ZHANG J J, XUE M. Study on GNSS-based detection technology of bistatic radar reflection signals of small satellites. Proc. of the 17th IEEE International Conference on Communication Technology, 2017: 1111–1115.

[22] ABE A, WALKER S D. Enhancement of 60 GHz transmission over 802.11ad using specular reflection. Proc. of the IEEE International Symposium on Local and Metropolitan Area Networks, 2016. DOI: 10.1109/LANMAN.2016.75

48859.
[23] CHEN D B, FAN Z K, HUANG H. Measurement of effective receiving area of open wave guide. High Power Laser and Particle Beam, 2004, 16(4): 474–476. (in Chinese)
[24] MARTIN J, MULGREW B. Analysis of the theoretical radar return signal form aircraft propeller blades. Proc. of the IEEE International Conference on Radar, 1990: 569–572.
[25] THEODORE R. Wireless communications: principles and practice. New Jersey: Prentice Hall, 1996.
[26] NORLAND R. Multipath of flat plate radar cross section measurements. Proc. of the International Conference on Radar, 2003: 152–155.
[27] ZHANG N T, MENG J. Reflection characteristics analysis of IR-UWB signal. Proc. of the 4th International Conference on Wireless Communications, Networking and Mobile Computing, 2008. DOI: 10.1109/WiCom.2008.265.
[28] SAVI P, BERTOLDO S, MILANI A. GNSS reflectometry systems for soil permittivity determination. Proc. of the 13th European Conference on Antennas and Propagation, 2019: 1–4.
[29] YANG D K, ZHANG Q S. Fundamentals and practice of GNSS reflection signal processing. Beijing: Electronic Industry Press, 2012. (in Chinese)
[30] HUANG F. Study on propagation characteristics and channel modeling of maritime radio waves. Hainan, China: Hainan University, 2015. (in Chinese)
[31] YANG Y, JING L. Impact of the metal permittivity on radar target scattering cross section. Laser & Infrared, 2013, 43(2): 155–158. (in Chinese)
[32] DAI Q W, LV S L, XIAO B. Discussion on application conditions of ground penetrating radar. Geophysical and Geochemical Exploration, 2000, 2(24): 157–160. (in Chinese)
[33] TSAI C C, CHIANG C T, LIAO W J. Radar cross section measurement of unmanned aerial vehicles. Proc. of the IEEE International Workshop on Electromagnetics: Applications and Student Innovation Competition, 2016. DOI: 10.1109/iWEM.2016.7504915.

Biographies

LI Xiaohui was born in 1972. She graduated from Xidian University with her B.S. degree in communication engineering in 1994. She received her M.S. degree in engineering from Xidian University in 2000. Since 2003, she has been engaged in research on MIMO OFDM wireless resource management technology. She received her Ph.D. degree in engineering in 2007 from Xidian University. She is a professor in Xidian University. Her research interests are broadband wireless communication and wireless resource management.
E-mail: xhli@mail.xidian.edu.cn

FANG Cong was born in 1996. He received his B.S. degree in information engineering from Xidian University in 2018. He is now studying at the School of Communication Engineering, Xidian University, majoring in electronics and communication engineering. His main research interests are detection of low-speed small aircraft, communication and information systems, and signal processing.
E-mail: xdufc@qq.com

FAN Tao was born in 1994. He received his B.S. degree from Xidian University in 2016. He is currently pursuing his Ph.D. degree with the State Key Laboratory on Integrated Services Network, Xidian University. His research interests include wireless communication, non-orthogonal multiple access, and millimeter wave channel estimation.
E-mail: 601391627@qq.com